Contents

Appendix E. Intruder Intersection Models

E.1. Small-Body Direct-Movement Intruder Intersection

Idea: There are *small intruders* which have body *smaller* than average $cell_{i,j,k}$ cell size. Its trajectory will stick to *linear trajectory* prediction with high probability.

Space Intersection Rate: The *Space Intersection Rate* for $cell_{i,j,k}$ is implemented as simple point cloud intersection. Where *sufficiently thick* point cloud is defined along *line* (eq. E.1):

$$position(time) = position(time_0) + velocity \times time, \quad time \in [0, \infty[\tag{E.1}$$

Then there exist projection function from local Euclidean coordinates to local polar coordinates (eq. E.2. The function projects intruder trajectory (eq. E.1) to planar coordinates $[distance, horizontal^\circ, vertical^\circ]$ as a set of sufficiently thick point cloud.

$$polarSet : position(t) \to \{[distance, horizontal^\circ], vertical^\circ\} \tag{E.2}$$

The *space intersection rating* $SpaceIntersection(\circ)$ for line type is given as (eq. E.3). If there exist non empty intersection of $polarSet \cap cell_{i,j,k}$ there is space intersection rate equal to 1, if intersection $polarSet \cap cell_{i,j,k} = \varnothing$ then the rate is zero.

$$space\begin{pmatrix} Intruder, \\ cell_{i,j,k} \end{pmatrix} = \begin{cases} 1: & \exists point \in polarSet(eq.E.2) : point \in c_{i,j,k} \\ 0: & \text{otherwise} \end{cases} \tag{E.3}$$

Note. The *intruder intersection rate* is multiplication of *space intersection rate* and time intersection rate. The *intersection rate* is calculated for *every intruder* and *selected intersection model* separately.

E.2. Notable-Body Direct-Movement Intruder Intersection

Idea: The *Intruder* has body volume greater than *average* $cell_{i,j,k}$ volume. The *intruder body* is considered as the ball moving along *intruder position*. The *intersection* of the intruder body is realized as sufficiently thick *point-cloud intersection*.

Space Intersection Rate - Body Volume: The *body volume mass* with center at *position*(t) is moving along intruder trajectory prediction (eq. E.4) in time interval $[0, \infty[$:

$$position(time) = position(time_0) + velocity \times time \tag{E.4}$$

The body *Volume ball* $Body(position(t), radius)$ (eq. E.5) is defined as set of points in $\mathbb{R}^3$ euclidean space. The center is moving along the *position(t)*. The body *volume ball* is a set of points sufficiently thick including also inner points. The *thickness* is guaranteed by existence of neighbour point which is close enough.

$$Body(position(t), radius) = \left\{ \begin{array}{r} ||position(t) - point|| \leq radius \\ point \in \mathbb{R}^3 : \forall point_i \exists point_{j \neq i}, \\ distance(point_i, point_j) \leq thickness \end{array} \right\} \tag{E.5}$$

The *polar volume ball polarBody* (eq. E.6) is projection of body volume ball set $Body(position(t), radius)$ to a set of planar coordinates in avoidance grid coordinate frame:

$$polarBall(t) : Body(position(t), radius) \rightarrow \left\{ \begin{bmatrix} distance, horizontal^{\circ}, \\ vertical^{\circ}, intersectionTime \end{bmatrix} \right\} \tag{E.6}$$

The *space intersection rate for vehicle body space*($Intruder, cell_{i,j,k}$) (eq. E.7) is calculated as intersection of polar body volume ball and $cell_{i,j,k}$. If intersection is non empty then base probability is one, zero otherwise:

$$space \begin{pmatrix} Intruder, \\ cell_{i,j,k} \end{pmatrix} = \begin{cases} 1: & \exists point \in polarBall(eq.E.6) : point \in c_{i,j,k} \\ 0: & \text{otherwise} \end{cases} \tag{E.7}$$

Intersection Time: The *intersection time* id depending on point cloud (eq. E.6) where each point *have intersection time* given as *body-center position* time (eq. E.4).

Note. The *body-volume* intersection model can insert the *multiple intersection times* into one $cell_{i,j,k}$. The *interval length* considers all of these for intersection rates (eq. **??**).

E.3. Maneuvering-Intruder-Intersection

Idea: The *intruders* are not bullets they are not sticking to predicted linear paths. The *intruder* maneuverability is given as horizontal and vertical spread. Therefore *intruder reach set* will form an *elliptic cone*. This cone can be transformed into *finite discrete* point-cloud, each *point* should have assigned *severity* impact value. The point cloud intersection with *Avoidance Grid* will give us space impact of an*uncertain* intruder.

Note. The following section will use condensed notation, due to the equation complexity. The *terminology* is consistent with the rest of the section.

Space Intersection Rate - Body Volume Intersection: $P_T(i_k(x_s, v, \theta, \phi), c_{i,j,k})$ computation is less straight-forward than other space intersection rates. First let us define the linear intruder i_k positions x at time t (eq. E.8) model, where $x(t)$ defines intruder position in *avoidance grid euclidean coordinate frame* at time t_i, v defines intruder velocity, and t is a time offset.

$$x(t) = x_s + v_I.t \tag{E.8}$$

Intruder *horizontal spread* θ and *vertical spread* ϕ are introduced. These spreads represents intruder deviation limits along from linear trajectory prediction $x(t) \in \mathbb{R}^3$. The example is given by (fig. E.1) where the intruder starts at point x_s with fixed velocity v, the linear trajectory prediction is outlined by blue line. The *predicted intruder position* at time $t = 10s$ is given by $x(10)$ (blue point). The ellipsoidal space $E(x)$ is projected on the plane $D(x(t))$. The plane D (eq. E.9) for point $x(t)$ and velocity v is defined as an orthogonal plane to velocity vector $v \in \mathbb{R}^3$ with origin at intruder position $x(t)$.

$$D(x(t), v) = \left\{a \in \mathbb{R}^3 : (a - x(t)) \perp v, \right\} \tag{E.9}$$

To construct ellipsoidal space boundary on orthogonal plane $D(x(t), v)$ some parameters are defined in (eq. E.10). The *scalar distance* $d_d x(t)$ is simple Euclidean norm, *maximal horizontal offset* $d_\theta(x_t)$ is given as product of sinus of horizontal offset angle θ and scalar distance d_d, and *maximal vertical offset* $d_\phi(x(t))$ is given a product of sinus of vertical offset angle ϕ and scalar distance d_d.

$$\begin{aligned} d_d &= d_d(x(t), x_s) = ||x(t) - x_s||_2 \\ d_{\theta_{\max}} &= d_\theta(x(t)) = \sin\theta(i_k).d_d(x(t)) \\ d_{\phi_{\max}} &= d_\phi(x(t)) = \sin\phi(i_k).d_d(x(t)) \end{aligned} \tag{E.10}$$

The *Ellipsoid* $E(x(t), v)$ (eq. E.11) for fixed intruder position $x(t)$ and fixed intruder velocity v is given as constrained portion of orthogonal plane $D(x(t), v)$. The constraint is defined by an internal coordinate frame $p \in \mathbb{R}^2$ which is space reduction of plane $D(x(t), v)$.

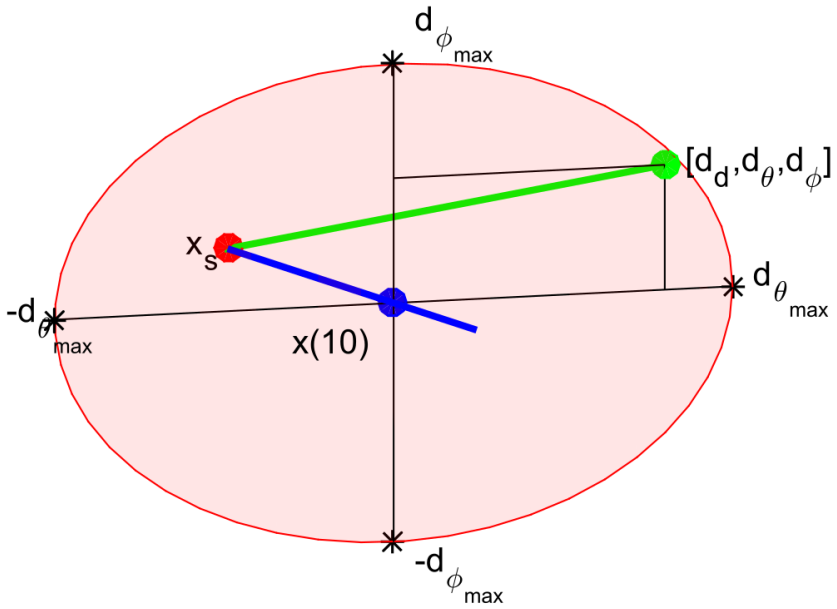

Figure E.1: One rate position $[d_d, d_\theta, d_\phi]$ (green). deviated from linear trajectory (blue line) at point $x(10)$.(blue) with initial position x_s (red)

The internal coordinate frame $p \in \mathbb{R}^2$ has origin in $x(t) \to \mathbb{R}^2$. The points of plane p are bounded by projection $p = (b - x(t)) \to \mathbb{R}^2$, where $b \in D(x(t), v)$. The point of ellipsoidal p is then given as standard ellipse boundary with vertical span $d_\theta(x(t))$ and horizontal span $d_\phi(x(t))$.

The 2D *Ellipsoid* $E(x(t), v)$ for specific time $t = 10s$ example is portrayed as red ellipsoid (in fig. E.1).

$$E(x(t), v) = \left\{ \begin{array}{c} b \in \mathbb{R}^3 : b \in D(x(t), v), p = (b - x(t)) \to \mathbb{R}^2, \\ \left(\frac{p(1)^2}{d_\theta(x(t))^2} + \frac{p(2)^2}{d_\phi(x(t))^2} \right) \leq 1 \end{array} \right\} \tag{E.11}$$

The expected behavior of an intruder i_k is to stick to predicted linear trajectory $x(t)$ (E.8). The probability of deviation should be decreasing with distance from the ellipse center (fig. E.2.). *Probability density function* for ellipsoid $E(x(t), v)$defined in (eq. E.11) is depending on maximal horizontal spread $d_\theta(x(t))$, maximal vertical spread $d_\phi(x(t))$, defined by (eq. E.10).

Two standard probabilistic distributions are established $\mathcal{N}(\mu_\theta, \sigma_\theta)$ (eq. E.12) for horizontal spread $\theta(x(t))$ and $\mathcal{N}(\mu_\phi, \sigma_\phi)$ (eq. E.13) for vertical spread $\phi(x(t))$. The means μ_θ and μ_ϕ are set to zero, and internal coordinate frame $p \in \mathbb{R}^2$ where $x(t) \to \mathbb{R}^2$ is frame center. The variances σ_θ and σ_ϕ are set as maximal distances on horizontal/vertical spread axes $d_\theta(x(t))$ and $d_\phi(x(t))$.

$$P(x(t), d_\theta) = \mathcal{N}(\mu_\theta, \sigma_\theta) = \mathcal{N}(0, d_\theta(x(t))) \tag{E.12}$$

$$P(x(t), d_\phi) = \mathcal{N}(\mu_\phi, \sigma_\phi) = \mathcal{N}(0, d_\phi(x(t))) \tag{E.13}$$

The combined *probability density function* for maximal spreads d_θ and d_ϕ is given by (eq. E.14). Because probability density function is defined for internal space $p \in \mathbb{R}^2$ and one may need to calculate impact rate for cell space $c_{i,j,k} \in \mathbb{R}^3$.

The reduction from two parameter probability distribution function to scalar rate distribution function is needed. A scalar rate distribution function $P(x(t), d_\theta, d_\phi)$ over ellipsoid $E(x(t), v)$ is

defined as (eq.E.14), where the final rate is given as an average of two partial probabilities.

Final space intersection rate $P(x(t), d_\theta, d_\phi)$ needs to be normalized to hold *normal distribution condition* (eq. E.15). Normal distribution condition value (eq. E.15) is given as surface integral over ellipsoid $E(x(0), v)$ with rate distribution function $P(x(t), d_\theta, d_\phi)$.

$$P(x(t), d_\theta, d_\phi) = \frac{\mathcal{N}(\mu_\theta, \sigma_\theta) + \mathcal{N}(\mu_\phi, \sigma_\phi)}{2} \tag{E.14}$$

$$\iint_{E(x(\tau))} P(x(t), d_\theta, d_\phi)\, \mathrm{d}d_\theta\, \mathrm{d}d_\phi = 1 \tag{E.15}$$

Final space intersection rate $P(x(t), c_{i,j,k}, \theta, \phi)$ (space portion, time portion is calculated in (eq.**??**) is given by (eq. E.17). Its mean value of all intersection rates $P(x(\tau), c_{i,j,k}, \theta, \phi)$ where $\tau \in [i_e(c_{i,j,k}), i_l(c_{i,j,k})]$ is fixed point in intersection time interval.

An $P(x(\tau), c_{i,j,k}, \theta, \phi)$ (E.16) is integration of rate density function $P(x(\tau), d_\theta, d_\phi)$ (eq. E.14) in surface $E(x(\tau), v)$ to cell $c_{i,j,k}$ volume intersection.

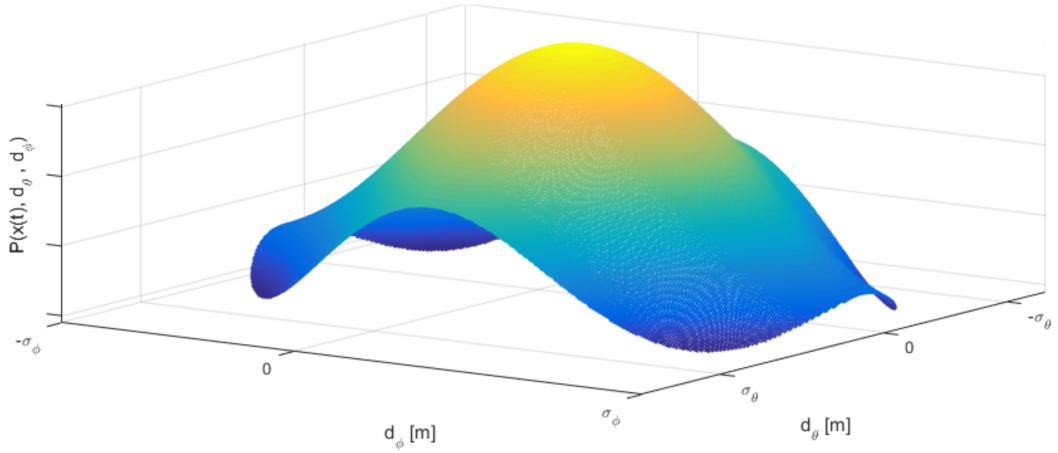

Figure E.2: Probability of intruder i_k position in ellipsoid $E(x(t), v)$

To get a volume integration partial rate in surface intersection must be integrated and normalized in time interval $\tau \in [i_e(c_{i,j,k}), i_l(c_{i,j,k})]$, the *base intersection probability* $P_T(i_k(x_s, v, \theta, \phi), c_{i,j,k})$ is given by (eq. E.17). Example of intersection of intruder i_r uncertain ellipsoid cone with avoidance grid $\mathcal{A}(t_i)$ is given in (fig. E.3).

$$P(x(\tau), c_{i,j,k}, \theta, \phi) = \iint_{E(x(\tau),v) \cap c_{i,j,k}} P(x(\tau), d_\theta, d_\phi) \tag{E.16}$$

$$P_T(i_k(x_s, v, \theta, \phi), c_{i,j,k}) = \frac{\int_{i_e(c_{i,j,k})}^{i_l(c_{i,j,k})} P(x(\tau), c_{i,j,k}, \theta, \phi)\, \mathrm{d}\tau}{i_l(c_{i,j,k}) - i_e(c_{i,j,k})} \tag{E.17}$$

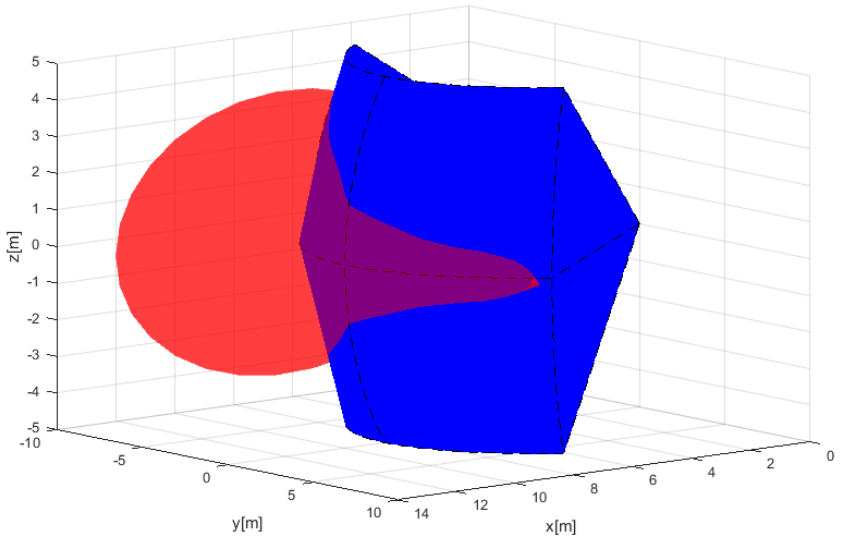

Figure E.3: Avoidance grid $\mathcal{A}(t_i)$ (blue) intersection with elliptic cone intruder $i_k(x, v, \theta, \phi)$ (red) example.

A *numeric approximation* of space intersection rate $P_T(i_k(x_s, v, \theta, \phi), c_{i,j,k})$ is more implementation feasible than symbolic calculation due to the multiple intersection constraints and bad intersection algorithm complexity.

Let us define a homogeneous discrete subset of real numbers $\mathcal{R}$ which is a non-empty subset of real numbers $\mathbb{R}$. The set $\mathcal{R}$ (eq. E.18) is homogeneous that means for an equal interval $(i, i+1], i \in \mathbb{Z}$ subset the count of members is equal to some positive natural number k. The parameter k can be understood as *unit approximation density*.

Similarly, the power sets $\mathcal{R}^2 \subset \mathbb{R}^2$, $\mathcal{R}^3 \subset \mathbb{R}^3$, ... $\mathcal{R}^i \subset \mathbb{R}^i, i \in \mathbb{N}^+$ keeps homogeneous distribution.

$$\mathcal{R} = \left\{ \begin{array}{c} a \in \mathbb{R} : \forall i \in \mathbb{Z}, |i < a \leq i+1| = k, k \in \mathbb{N}^+, \\ \forall j \in \mathbb{N}^+ a_{j+1} - a_j = m, m \in \mathbb{R}^+ \end{array} \right\}, \mathcal{R} \subset \mathbb{R} \tag{E.18}$$

The orthogonal plane for $x(t), v, t \in \mathbb{R}$ is defined by (eq. E.9). The orthogonality property is also kept for any subspace $\mathcal{R}^n \in \mathbb{R}^n, n \in \mathbb{N}^+$. Numeric approximation of $D(x(t), v)$ is given as $D_D(x(t), v)$ (eq. E.19).

The only difference is that discrete approximation is countable $|D_D| = m, m \in \mathbb{N}^+$, but continuous representation $|D| \approx \infty$ is uncountable. Because ellipsoid is a subset of orthogonal plane it keeps its countability property; therefore E_D is also countable and must contain at least one member.

$$D_D(x(t), v) = \left\{ a \in \mathcal{R}^3 : (a - x(t)) \perp v, \right\}, t \in \mathcal{R} \tag{E.19}$$

The *base ellipsoid* $E(x(t), v)$ for continuous-space is given by (eq. E.11). Every element, expect the base of internal projection $\mathcal{R}^2$ and orthogonal plane D_D is same in discrete case $E_D(x(t), v)$ (eq. E.20).

$$\bar{E}_D(x(t), v) = \left\{ \begin{matrix} b \in \mathcal{R}^3 : b \in D_D(x(t), v), p = (b - x(t)) \rightarrow \mathcal{R}^2, \\ \left(\frac{p(1)^2}{d_\theta(x(t))^2} + \frac{p(2)^2}{d_\phi(x(t))^2} \right) \leq 1 \end{matrix} \right\}, t \in \mathcal{R} \tag{E.20}$$

The *numeric calculation disproportion* can occur in case that ellipsoid $\bar{E}_D(x(t), v)$ (E.20) in case of $d_\theta(x(t)) \approx 0$ and $d_\phi(x(t)) \approx 0$. The count of ellipsoid members can be $|\bar{E}_D(x(t), v)| = 0$, which is in contradiction with assumption $|\bar{E}_D(x(t), v)| \neq 0$.

Let assume for discrete times $\tau = \{t_1, t_2, \ldots, t_i\}$, $i \in \mathbb{N}^+$ there exists ellipsoids $\bar{E}_D(x(t_1), v)$,$\bar{E}_D(x(t_1), v)$, $\ldots$, $\bar{E}_D(x(t_i), v)$ which are non empty and in space $\mathcal{R}^2$ in internal coordinate frame and space $\mathcal{R}^3$ in avoidance grid $\mathcal{A}(t_i)$ coordinate frame. The intersection of these partial ellipsoids in both spaces is equal to:

$$\bar{E}_D(x(t_1), v) \cap \bar{E}_D(x(t_2), v) \cdots \cap \ldots \bar{E}_D(x(t_i), v) = \varnothing \tag{E.21}$$

An *empty intersection* enables us to keep homogeneity property of ellipsoids by adding points so it is safe to add specific point $x(t)$ into empty ellipsoid. But only one, because it does not impact probability density functions $\mathcal{N}(\mu_\theta, \sigma_\theta)$ and $\mathcal{N}(\mu_\phi, \sigma_\phi)$, neither space intersection rate density function $P(x, d_\theta, d_\phi)$.

The final ellipsoid used forward $E_D(x(t), v)$(eq. E.22) is keeping all properties of ellipsoid $E(x(t), v)$ (eq. E.22).

$$E_D(x(t), v) = \begin{cases} |\bar{E}_D(x(t), v)| = 0 & : \{x(t)\} \\ |\bar{E}_D(x(t), v)| \geq 0 & : \bar{E}_D(x(t), v) \end{cases} \tag{E.22}$$

The normal distribution condition for rate distribution function $P_D(x(t), d_\theta, d_\phi, p)$, which is instance of to rate density function $P(x(y), d_\theta, d_\phi)$ (eq. E.14) is used. This rate distribution must be normalized according to (eq. E.23).

$$\sum_{p \in \bar{E}_D(x(t))} P_D(x(t), d_\theta, d_\phi, p) = 1, \forall t \in \mathcal{R}^+ \tag{E.23}$$

The equations for *space intersection rate* are similar to (eq. E.16, E.17). For cell $c_{i,j,k}$ there exist intruder entry time $i_e(c_{i,j,k})$ its the earliest intersection with ellipsoid $E_D(x(i_e(c_{i,j,k}))), v$. Same situation occurs with intruder leave time $i_l(c_i, j, k)$. Because E_D is countable set, it means additional attributes can be attached to each point $p \in E_D$. Based on system dynamic (eq. **??**) the *Time Of Arrival* (TOA) can be calculated. The example of TOA is given in fig. E.4.

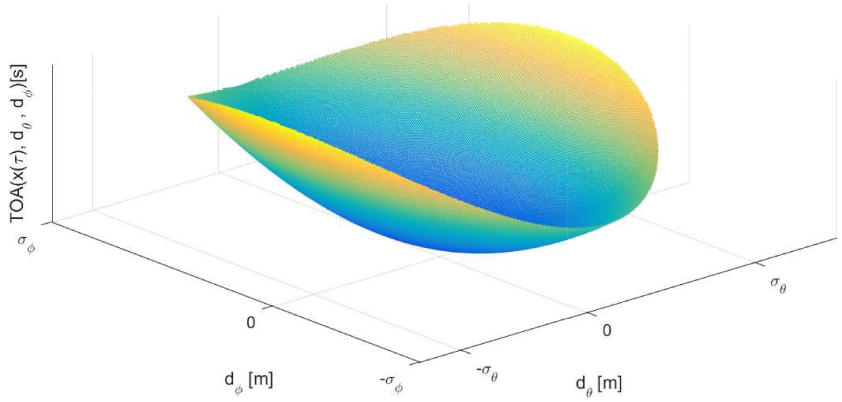

Figure E.4: Time Of Arrival (TOA) for one ellipsoid $E_D(x(\tau), v)$.

The intersection rate $P_D(x(\tau), c_{i,j,k}, \theta, \phi)$ for one time sample τ is given by (eq. E.24), which has similar notation to (eq. E.16), sums are used instead of integrals and discrete rate density function $P_D(x(\tau), d_\theta, d_\phi, p)$ for points form ellipse and cell intersection are used as iterator base set $p \in \{E_D(x(\tau), v) \cap c_{i,j,k}\}$.

$$P_D(x(\tau), c_{i,j,k}, \theta, \phi) = \sum_{p \in \{E_D(x(\tau), v) \cap c_{i,j,k}\}} P_D(x(\tau), d_\theta, d_\phi, p) \tag{E.24}$$

The *space intersection rate* $P_{TD}(i_k(x_s, v, \theta, \phi), c_{i,j,k})$ (eq. E.25) is given as mean intersection rate of partial intersections $P_D(x(\tau), c_{i,j,k}, \theta, \phi)$ where step set $T = \{ i_e(c_{i,j,k}), \ldots, i_l(c_{i,j,k})\}$ contains all viable intersection times with ellipsoids $E(x(\tau \in T), v)$. The denominator is basically count of samples in sample time set T.

$$P_{TD}(i_k(x_s, v, \theta, \phi), c_{i,j,k}) = \frac{\sum_{\tau=i_e(c_{i,j,k})}^{i_l(c_{i,j,k})} \sum_{p \in E_D(x(\tau), v)} P_D(x(\tau), c_{i,j,k}, \theta, \phi, p)}{\sum_{\tau i_l(c_{i,j,k})}^{i_e(c_{i,j,k})} 1} \tag{E.25}$$

An *intersection of intruder cone and cell* $c_{i,j,k}$ cell is defined by (eq. E.26) The set of point $p \in \mathcal{R}^3$ where condition of intersection between ellipsoids $E_D(x(\tau), v)$ for times $\tau \in \mathcal{R}^+$ and cell space $c_{i,j,k}$ is met.

$$\mathcal{P}(i_k(x_s, v, \theta, \phi), c_{i,j,k}) = \bigcup_{\forall \tau \in \mathcal{R}^+} \left\{ p \in \mathcal{R}^3 : p \in c_{i,j,k} \cap E_D(x(\tau), v) \right\} \tag{E.26}$$

An *intruder time of entry* $i_e(i_k, c_{i,j,k})$ (eq. E.27), for intruder i, k and cell $c_{i,j,k}$ is approximated for discrete point set $\mathcal{P}(i_k(x_s, v, \theta, \phi), c_{i,j,k})$ (eq. E.26) as minimal time of arrival $t_{TOA}(p)$ of member points p.

$$i_e(i_k, c_{i,j,k}) \approx \min \left\{ t_{TOA}(p) : p \in \mathcal{P}(i_k(x_s, v, \theta, \phi), c_{i,j,k}) \right\} \tag{E.27}$$

An *intruder time of leave* $i_l(i_k, c_{i,j,k})$ (eq. E.28), for intruder i, k and cell $c_{i,j,k}$ is approximated for discrete point set $\mathcal{P}(i_k(x_s, v, \theta, \phi), c_{i,j,k})$ (eq. E.26) as maximal time of arrival $t_{TOA}(p)$ of member points p.

$$i_l(i_k, c_{i,j,k}) \approx \max \left\{ t_{TOA}(p) : p \in \mathcal{P}(i_k(x_s, v, \theta, \phi), c_{i,j,k}) \right\} \tag{E.28}$$

Combined intersection model: The *combined intersection model* $P_{O_l}(i_k, c_{i,j,k}, l, b, s, \tau)$ is defined for intruder i_k with parameters:

1. *Starting position* x_s - expected position of intruder i_r in 3D space at time of avoidance t_i in avoidance grid frame $\mathcal{A}(t_i)$.

2. *Velocity vector* v - oriented velocity of intruder i_r at time of avoidance t_i in avoidance grid frame $\mathcal{A}(t_i)$.

3. *Horizontal uncertainty spread* θ - defines how much can intruder i_r deviate on horizontal axis of intruder local coordinate frame (if X+ is the main axis, then Y is horizontal axis in right-hand euclidean coordinate frame), due the properties of intersection definition, the horizontal uncertainty spread can have following values $\theta \in [0, \pi/2]$.

4. *Vertical uncertainty spread* ϕ -defines how much can intruder i_r deviate on vertical axis of intruder local coordinate frame (if X+ is the main axis in local right-hand euclidean intruder coordinate frame, then Z is horizontal-vertical axis), due to the intersection definition, the vertical uncertainty spread can have following values $\phi \in [0, \pi/2]$.

5. *Body volume radius* r - defines the body volume of an intruder in meters and it has $\mathbb{R}^+$ value.

The *flag vector* $l, b, s, \tau \in \{0, 1\}$ is a parametrization of rate calculation: l stands for the *lined intersection*, b stands for *body intersection*, s stands for the *spread intersection*, τ stands for *time account*.

The *space intersection for line* $P_L(i_k, c_{i,j,k})$ is defined as $P_T(i_k(x, v), c_{i,j,k})$, where i_k is intruder with properties of initial position x, velocity vector v and $c_{i,j,k}$ is target cell. (eq. E.3).

The *space intersection rate for body volume* $P_B(i_k, c_{i,j,k})$ is defined as $P_T(i_k(x, v, r), c_{i,j,k})$ (eq. E.7), where intruder i_r has additional property of the intruder body volume radius r.

The *space intersection probability for maneuverability uncertainty* $P_S(i_k, c_{i,j,k})$ is defined as $P_{TD}(i_k(x_s, v, \theta, \phi), c_{i,j,k})$ (eq. E.25), where intruder properties θ, ϕ stands for intruder horizontal and vertical uncertainty spread.

The *time intersection rate* $P_{\tau,x}(i_k, c_{i,j,k}) \in [0, 1]$ is defined in (eq. **??**). This probability has two calculation modes, first is for 1D intersection (line), second is for volume intersection (body volume, spread elliptic cone).

UAS cell entry time t_e and cell leave time t_l time for a vehicle in avoidance grid $\mathcal{A}(t_i)$ is given by (eq. **??**) and (eq. **??**).

Intruder leave and entry time for 1D intersections is trivial and is omitted in this section. Intruder entry i_e and intruder leave i_l for 3D intersection is given by (eq. E.27, E.28).

All partial rates with respective definition references are summarized in (eq. E.29)

$$
\begin{aligned}
P_L(i_k, c_{i,j,k}) &= P_T(i_k(x, v), c_{i,j,k}) && (E.3)\\
P_B(i_k, c_{i,j,k}) &= P_T(i_k(x, v, r), c_{i,j,k}) && (E.7)\\
P_S(i_k, c_{i,j,k}) &= P_{TD}(i_k(x_s, v, \theta, \phi), c_{i,j,k}) && (E.25)\\
P_{\tau,x}(i_k, c_{i,j,k}) &= \frac{\left|\left|[i_e(c_{i,j,k}), i_l(c_{i,j,k})] \cap [t_e, t_l]\right|\right|}{||[t_e, t_l]||} && (??)
\end{aligned}
\tag{E.29}
$$

With definition of all space and time intersection rates (eq. E.29) and given flag vector $l, b, s, \tau \in \{0,1\}$ one can formulate combined intersection rate $P_{O_l}(i_k, c_{i,j,k}, l, b, s, \tau)$ (eq. E.30) for intruder i_k and cell $c_{i,j,k}$. The principle is following: *maximum of selected rates product based on flag vector is final intersection rate of intruder i_k in the cell*.

The time-use flag τ is adding time intersection rate $P_{\tau,x}(i_k, c_{i,j,k})$, where time intersection rate is defined by $x = \{L, B, S\}$ for line, body volume, spread ellipse time intersections ($P_{\tau,L}(i_k, c_{i,j,k}) \neq P_{\tau,B}(i_k, c_{i,j,k}) \neq P_{\tau,B}(i_k, c_{i,j,k})$ for one intruder i_k).

$$P_{O_l}(i_k, c_{i,j,k}, l, b, s, \tau) = \begin{cases} \tau = 0 & : \max \begin{Bmatrix} P_L(i_k, c_{i,j,k}).l \\ P_B(i_k, c_{i,j,k}).b \\ P_S(i_k, c_{i,j,k}).s \end{Bmatrix} \\ \tau = 1 & : \max \begin{Bmatrix} P_{\tau,L}(i_k, c_{i,j,k}).P_L(i_k, c_{i,j,k}).l \\ P_{\tau,B}(i_k, c_{i,j,k}).P_B(i_k, c_{i,j,k}).b \\ P_{\tau,S}(i_k, c_{i,j,k}).P_S(i_k, c_{i,j,k}).s \end{Bmatrix} \end{cases} \tag{E.30}$$

Bibliography